Journal of the Association of Arab Universities for Basic and Applied Sciences (2014) **15**, 35–42

University of Bahrain

Journal of the Association of Arab Universities for Basic and Applied Sciences

www.elsevier.com/locate/jaaubas
www.sciencedirect.com

ORIGINAL ARTICLE

Synthesis and characterization of zeolite A by hydrothermal transformation of natural Jordanian kaolin

Mousa Gougazeh [a,*], **J.-Ch. Buhl** [b]

[a] *Natural Resources and Chemical Engineering Department, Faculty of Engineering, Tafila Technical University, P.O. Box 179 Tafila 66110, Jordan*
[b] *Institute of Mineralogy, Leibniz University Hannover, Callinstr. 3, D-30167 Hannover, Germany*

Received 6 March 2012; revised 4 March 2013; accepted 31 March 2013
Available online 29 April 2013

KEYWORDS

Zeolite A;
Kaolin;
Metakaolin;
Hydrothermal synthesis;
Hydroxysodalite

Abstract The synthesis of zeolite materials by hydrothermal transformation of natural Jordanian kaolin in NaOH solutions of various concentrations was investigated at 100 °C for 20 h. A mixture of zeolite A, quartz and hydroxysodalite (HS) was obtained. Zeolite A was the main product with the NaOH concentrations of 1.50–3.50 M, which was confirmed by XRD, IR and SEM. Zeolite A can be obtained from natural kaolin under the conditions applied showing that metakaolinization can be observed at 650 °C which is much lower than the temperatures given in the previous works, 700–950 °C. The products obtained from the experiments were characterized by X-ray diffraction (XRD), Fourier transform infrared spectroscopy (FTIR) and scanning electron microscopy (SEM).

1. Introduction

Zeolites are crystalline, microporous, hydrated aluminosilicates of alkaline or alkaline earth metals. The frameworks are composed of $[SiO_4]^{4-}$ and $[AlO_4]^{5-}$ tetrahedra, which corner-share to form different open structures. Negative charge of lattice is compensated by the positive charge of cations located at specific positions of zeolite framework (Bekkum et al., 1991; Breck, 1974). In most of zeolites the compensating cations are usually mono- and bi-valent metal ions and/or their combinations (Engelhardt and Michel, 1987; Takaishi et al., 1995; Earl and Deem, 2006). In accordance with the Loewenstein's rule (Loewenstein, 1954), Al–O–Al bonds do not exist in aluminosilicate frameworks of zeolite. Instead of the tetrahedrally bonded atoms Si and Al, so-called "T-atoms", others such as P, Ga, Ge, B, Be, etc. can exist in the framework as well (McCusker and Baerlocher, 2001; Takaishi et al., 1995).

The synthesis of zeolites in forms suitable for industrial applications is of great importance. The first synthesis of

* Corresponding author. Tel.: +962 776731158.
E-mail addresses: dr_eng_mhag@yahoo.com (M. Gougazeh), j.buhl@mineralogie.uni-hannover.de (J.-Ch. Buhl).
Peer review under responsibility of University of Bahrain.

Production and hosting by Elsevier

1815-3852 © 2013 Production and hosting by Elsevier B.V. on behalf of University of Bahrain.
http://dx.doi.org/10.1016/j.jaubas.2013.03.007

zeolite was attempted by St. Claire-Deville in 1862. Barrer's pioneering work in 1948 demonstrated that a wide range of zeolites could be synthesized from aluminosilicate gels.

At present, synthetic zeolites are used commercially more often than natural zeolites due to the purity of crystalline products and the uniformity of particle sizes (Breck, 1974; Szoztak, 1998). However, the preparation of synthetic zeolites from chemical sources of silica and alumina is expensive. Such costs may be reduced by the use of clay minerals, volcanic glasses (perlite and pumice), rice husks, diatoms, fly ash or paper sludge ash as starting materials (Adamczyk and Bialecka, 2005; Querol et al., 1997; Saija et al., 1983; Tanaka et al., 2004; Walek et al., 2008; Wang et al., 2008). Zeolite has also been developed by the transformation of one zeolite type into other zeotypes (Rios et al., 2007; Sandoval et al., 2009).

Previous work has shown that kaolin is not stable under highly alkaline conditions and different zeolitic materials can form, and that kaolin is usually used after calcinations to obtain a more reactive phase (metakaolin). After dehydration (endothermic dehydroxylation), kaolin is transformed into amorphous metakaolin (Fialips, 1999; Gougazeh and Buhl, 2010; Smykatz-Kloss, 1975). Raw kaolin and metakaolin have been used as the Al and Si sources for synthesis of zeolite Linde Type A, X, Y, P, 4A, NaA, KI, cancrinite, sodalite, hydroxysodalite, faujasite, phillipsite, chabazite and several other types of zeolites (e.g., Akolekar et al., 1997; Alberti et al., 1994; Barnes et al., 1999a, 1999b, 1999c; Bauer and Berger, 1998; Bauer et al., 1998; Buhl, 1991; Buhl et al., 2000a,b; Buhl and Loens, 1996; Covarrubias et al., 2006; Dudzik and Kowalak, 1974; Gualtieri et al., 1997; Lin et al., 2004; Loiola et al., 2012; Marcelo et al., 2007; Mon et al., 2005; Rees and Chandrasekhar, 1993; Sanhueza et al., 1999; Vilma et al., 1999; Zhao et al., 2004.

NaA Zeolite is of great industrial importance due to its molecular sieving, ion exchange and water adsorption properties. With the molar ratio Si/Al nearly equal to one, kaolin is an ideal raw material for preparing NaA zeolite. Kaolin was one of the most versatile industrial minerals and was used extensively for many applications (Murray, 1991). The synthesis of NaA zeolite from kaolin source was started from the 1970s (Breck, 1974; Barrer, 1978) by the hydrothermal reaction of dehydroxylated kaolin with sodium hydroxide solution.

No attempt has been made previously to produce zeolite type A from natural Jordanian kaolin. In this work, Zeolite A was hydrothermally synthesized from Jordanian kaolin, and the effect of NaOH concentration (1.0, 1.5, 2.0, 2.5, 3.5 and 4 M NaOH) was investigated. The synthesized products were characterized by X-ray diffraction (XRD) scanning electron microscopy (SEM) and Fourier transform infrared (FT-IR) spectroscopy.

2. Experimental

2.1. Raw materials and chemical reagent

The natural well crystallized kaolin (a combined source for silica and alumina), from the kaolin deposits in south Jordan (Gougazeh and Buhl, 2010) was used for the present study. The sodium hydroxide used was of analytical grade. Properties of Jordanian kaolin are shown in Table 1. Metakaolin was obtained by calcining kaolin in a muffle furnace at 650 °C for 2 h.

Table 1 Properties of natural Jordanian kaolin.

Chemical constituents in wt.% [X-ray fluorescence analysis (XRF)]	
SiO_2	53.86
TiO_2	0.74
Al_2O_3	32.45
Fe_2O_3	0.65
MnO	0.01
MgO	0.08
CaO	0.13
Na_2O	0.06
K_2O	0.54
P_2O_5	0.12
Loss on ignition (LOI)	11.21
Total	99.85
SiO_2/Al_2O_3 ratio	1.65
Particle size distribution in wt.% [Atterberg method]	
Microns 63–45 μm	1.2
Microns −45 + 6 μm	5.2
Microns −6 + 2 μm	20.6
Microns −2 μm	73.0
Quantitative analysis in wt.% [using XRD (Rietveld method with DIFFRAC$_{plus}$ TOPAS software) + XRF]	
Kaolin	72.0
Quartz	27.0
Others	1 .0
Brightness (% ISO)	82.73

2.2. Hydrothermal synthesis

Metakaolins were separately mixed with NaOH solutions of various concentrations, 1.0, 1.5, 2.0, 2.5, 3.0, 3.5 and 4.0 M. The samples were initially gently stirred for 10 min at room temperature for homogenization. The solid/liquid ratio of metakaolin to alkaline solution was 1.0 g/25 ml. The reaction mixtures were prepared separately with gentle stirring and then distributed among the required number of autoclaves. The autoclaves were kept in a conventional air oven at 100 °C for 20 h at autogenous pressure. The synthesized products were washed with distilled water three times and then dried at 80 °C for 24 h.

2.3. Characterization techniques

The original kaolin sample was dispersed in deionized water and shaken mechanically and then sieved through a 63 μm sieve. The portion of the <63 μm fraction (~98 wt.% of the original kaolin sample) was allowed to settle in an Atterberg cylinder according to Stock's law (Jachson, 1975) to separate the size fractions of 63–45 μm, 45–6 μm, 6–2 μm and <2 μm (Gougazeh and Buhl, 2010).

The chemical composition of kaolin was determined using a Bruker S4 wavelength X-ray dispersive fluorescence spectrometer (WDXRFS), with a Rh X-ray tube. Phase characterization was carried out by X-ray diffraction (XRD) using a Bruker AXS D4 ENDEAVOR diffractometer using Ni filtered Cu $K\alpha$ radiation at 40 kV and 40 mA. The measurements were carried out with a step width of 0.03° 2θ and scan rate of 1 s per step. The diffraction data were analyzed by the Rietveld method using DIFFRAC$_{plus}$ TOPAS software. Fourier transform infrared spectra (FTIR) were obtained by using a Bruker IFS66v FTIR spectrometer in 4000–400 cm^{-1} regions by the KBr wafer technique. The morphology was characterized by

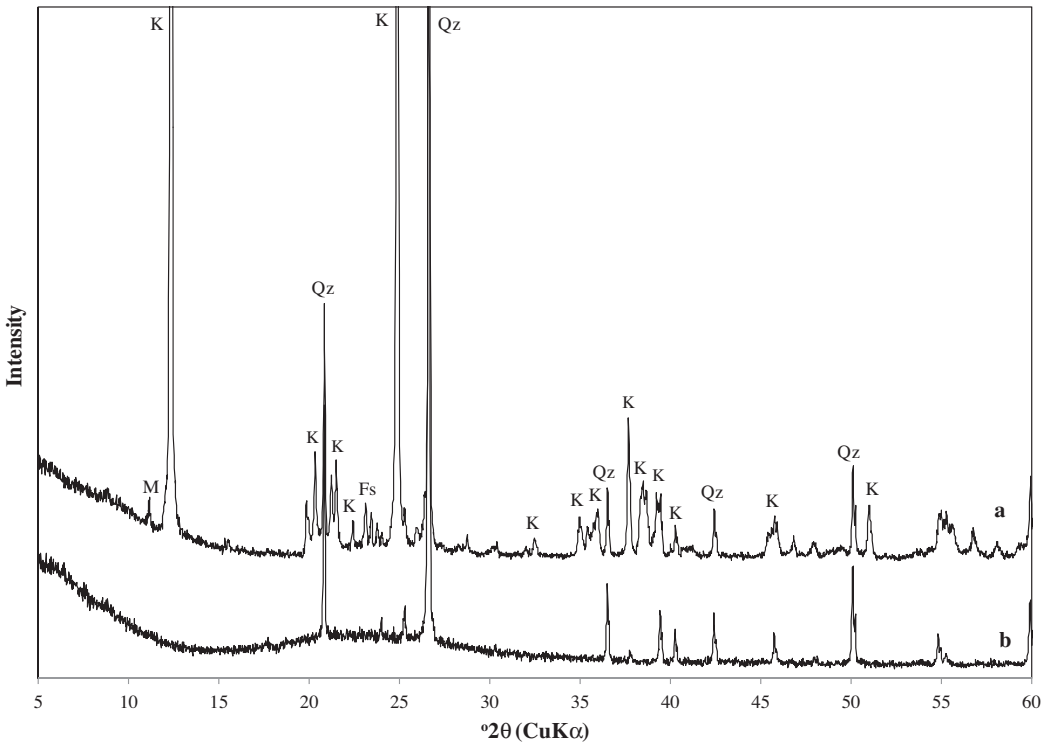

Figure 1 XRD patterns of Jordanian kaolin (a) and metakaolin at 650 °C (b).

a scanning electron microscope (SEM) at 20 kV, using a JEOL JSM-6390A model.

3. Results and discussion

The kaolin used was fully characterized (mineralogical and chemical composition, thermal behavior, particle size distribution, and so on) in previous study (Gougazeh and Buhl, 2010). The grain size analysis of bulk kaolin sample was separated by Atterberg methods. The quantitative analysis of the mineral content of the natural Jordanian kaolin has been worked out by a combination of XRD (Rietveld method using DIFFRAC$_{plus}$ TOPAS software) and XRF investigations (Gougazeh and Buhl, 2010).

The physical, chemical and mineralogical properties of the kaolin under study are presented in Table 1.

The SiO_2/Al_2O_3 ratio is found to be 1.65. The properties of the reaction intermediates and products were determined by various techniques to give the following results.

3.1. X-ray diffraction analysis

The XRD patterns of the natural (unheated) kaolin and metakaolin are shown in Fig. 1. In accordance with XRD data, the starting material contains 72 wt.% of kaolin, 27 wt.% of quartz and minor amount (about 1 wt.%) of other components (see Table 1). Kaolinite is identified by its characteristic X-ray diffraction peaks at 12.34° and 24.64° 2θ as has been reported in previous studies (Gougazeh and Buhl, 2010; Zhao et al., 2004). The XRD pattern of metakaolin obtained by heating the kaolin for 3 h at 650 °C resembled others, except for the peaks due to admixed impurities. After thermal treatment, the XRD patterns exhibit a significant change in comparison to the pattern of untreated kaolin, which was characterized by disappearance of the diffraction peaks of kaolin, accompanied by the appearance of amorphous aluminosilicate. Metakaolin is of amorphous structure and the highest diffraction peaks correspond to the presence of quartz (SiO_2), which is very common (Fig. 1b). The only crystalline phase in metakaolin is quartz. Therefore, the activation of kaolin produces structural changes of this mineral, promoting its reactivity to synthesize zeolitic materials.

The phase composition of the synthesized zeolite material which was obtained from the activated kaolin samples reacted with 1.0, 1.5, 2.0, 2.5, 3.0, 3.5 and 4.0 NaOH solutions was analyzed by X-ray diffractometry (XRD). Quantitative analysis of the obtained zeolite products was performed using the Rietveld method with DIFFRAC$_{plus}$ TOPAS software and the exact percentage of each phase was calculated (Table 2). The results suggest that the synthesized zeolite products contain zeolite A as the major constituent phase, whereas

Table 2 Phase composition of the obtained zeolite products (wt.%) was performed using the Rietveld method with DIFFRAC$_{plus}$ TOPAS software.

NaOH(M)	Quartz	Hydroxysodalite (HS)	Zeolite A	Metakaolin (amorphous)	Total
1.0	30.2	0.0	39.7	30.1	100.0
1.5	25.6	4.2	70.2	0.0	100.0
2.0	24.3	3.8	71.9	0.0	100.0
2.5	18.0	7.8	74.2	0.0	100.0
3.0	16.9	8.5	74.6	0.0	100.0
3.5	16.3	15.4	68.2	0.0	100.0
4.0	15.4	33.8	50.8	0.0	100.0

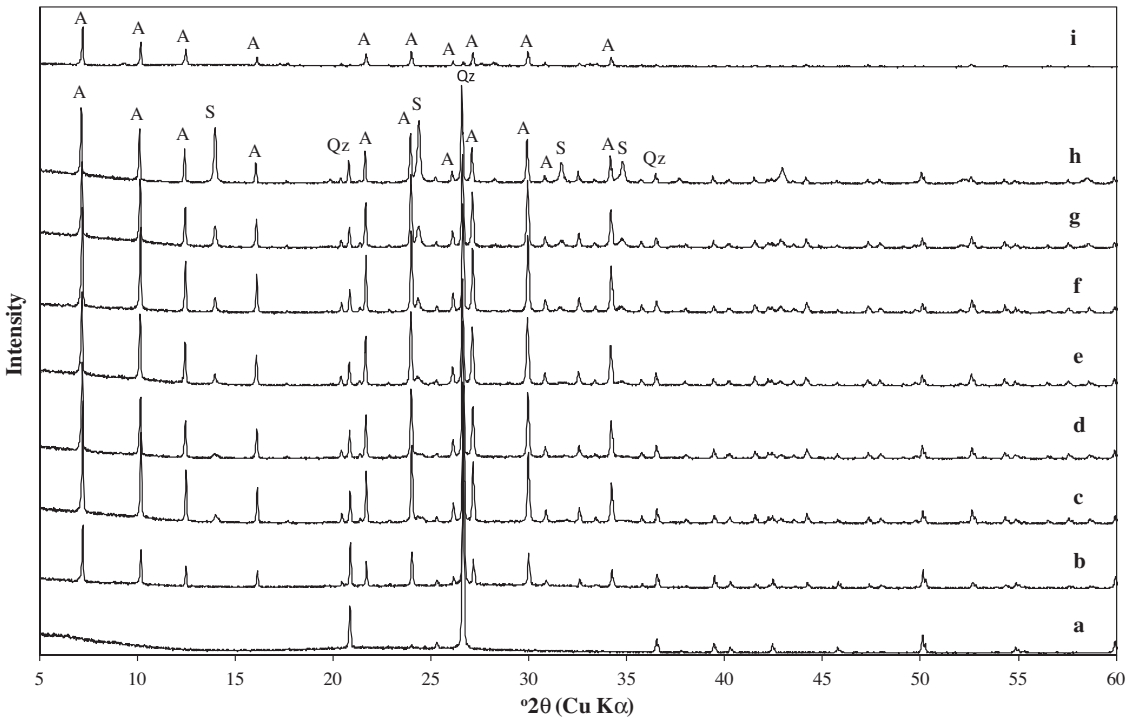

Figure 2 XRD patterns of zeolite A and associated phases obtained by hydrothermal synthesis (a) unreacted metakaolin, (b) 1.0 M NaOH, (c) 1.5 M NaOH, (d) 2.0 M NaOH, (e) 2.5 M NaOH, (f) 3.0 M NaOH, (g) 3.5 M NaOH, and (h) 4.0 M NaOH, (i) commercial zeolite A. A: zeolite A, S: hydroxysodalite, Qz: quartz.

hydroxysodalite (HS) and quartz were found as minor phases (Table 2).

Fig. 2 illustrates the X-ray powder diagrams of metakaolin and the reaction products which were obtained from the activated kaolin samples reacted with 1.0, 1.5, 2.0, 2.5, 3.0, 3.5 and 4.0 M NaOH solutions at 100 °C for 20 h and the commercial zeolite A sample (Fluka No. 69836) given for comparison. The formation of synthesized zeolite A in the products was detected, by comparing the d-values of the products obtained with JCPDS (Joint Committee on Powder Diffraction Standards) data of card No.: 39-222 and d-values of commercial zeolite A sample. The most important change observed in the XRD patterns is the appearance of the characteristic peaks of zeolite A. The synthesized products matched the characteristic peaks of zeolite A at 2θ values of 7.2°, 10.3°, 12.6°, 16.2°, 21.8°, 24°, 26.2°, 27.2°, 30°, 30.9°, 31.1°, 32.6°, 33.4° and 34.3° that were reported by Treacy and Higgins (2001). Fig. 2b shows the XRD pattern of the reaction product which was obtained from the thermally activated kaolin sample with 1.0 M NaOH solution, zeolite A and quartz were determined as the dominant mineral phases with a significant amount of metakaolin (amorphous) and no hydroxysodalite was observed (Table 2). The results indicated that the synthesized zeolite products obtained from 1.5–3.5 M NaOH concentrations contain zeolite A as the major constituent phase, whereas hydroxysodalite (HS) and quartz were found as minor phases (Fig. 2c–h). According to the experimental results and the XRD data, intensities of the HS peaks in the pattern increase with increasing NaOH concentration (Table 2 and Fig. 2). Fig. 2 and Table 2 show that the greatest quantities of formed zeolite A are essentially the same for the samples reacted with NaOH concentration between 1.5 and 3.5 M (zeolite A persisted as the dominant phase) (Fig. 2c–g), with a sudden decrease at higher base concentrations (> 3.5 M) (Fig. 2h), during this reaction some zeolite A was converted into hydroxysodalite. Similar observations were made by Singer and Berkgaut, 1995, Lin and His, 2004, Querol et al., 1997 who found that zeolite A was formed at low base concentrations (< 3.5 M) and HS at higher base concentrations. Hydroxysodalite shows several common peaks located at 13.96°, 19.98°, 24.42°, and 35.00°. Our results showed that quartz was also observed in the synthesized zeolitic material in a minor amount (Table 2).

3.2. FTIR analysis

Fig. 3 illustrates the IR spectra of the unreacted and reacted metakaolin in various alkalinities and the commercial zeolite A sample (Fluka No. 69836) given for comparison. The broad band of metakaolin in the spectral range from about 925 cm^{-1} to about 690 cm^{-1} (spectrum a in Fig. 3), assigned to Al–O bonds in Al_2O_3 does not appear in the zeolite products (spectra b–g in Fig. 3). The 1080 cm^{-1} band of metakaolin was shifted to 1000 cm^{-1} (1035, 1004, 1003, 1001, 1000 and 996 cm^{-1}) (Fig. 3b–h), which could be assigned to antisymmetric stretching of T–O bonds (T = Si or Al) in aluminosilicates with zeolite structure. SiO_2 and Al_2O_3 are transformed to aluminosilicates during the reaction between metakaolin and NaOH. Their vibration bands in the IR spectrum are replaced by a single band around 1000 cm^{-1}, characteristic of Si–O–Al bonds in TO_4 tetrahedra (Nesse, 2000). A broad band of week intensity, is observed around 553 cm^{-1}, this peak indicates the presence of zeolite A band assigning the cubic prism. The band at 553 cm^{-1} could represent the beginning of the crystallization

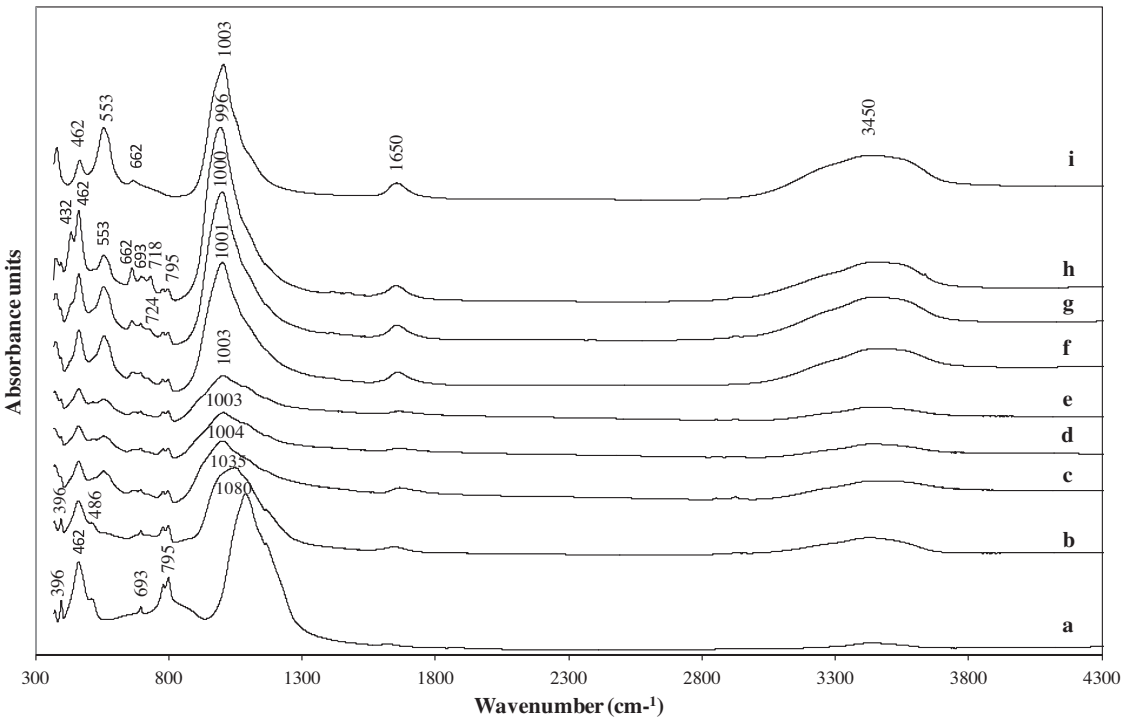

Figure 3 FTIR spectra of zeolite A and associated phases obtained by hydrothermal synthesis: (a) unreacted metakaolin, (b) 1.0 M NaOH, (c) 1.5 M NaOH, (d) 2.0 M NaOH, (e) 2.5 M NaOH, (f) 3.0 M NaOH, (g) 3.5 M NaOH, (h) 4.0 M NaOH, and (i) commercial zeolite A (Fluka No. 69836).

of a zeolite with double rings (Alkan et al., 2005). The bands at 462 and 662 cm^{-1} are close to the bands at 462 and 668 cm^{-1}, which correspond to the internal linkage vibrations of the TO_4 (T = Si or Al) tetrahedra and to the asymmetric stretching, respectively, of zeolite A.

There are four well-defined peaks at 662, 693, 718 and 724 cm^{-1} in the spectral zone of 650–745 cm^{-1} (Fig. 3b–h) assigned to symmetric T–O–T vibrations of the sodalite framework in good agreement with the peaks of 660, 701 and 729 cm^{-1} for hydroxysodalite zeolite reported by Flaningen et al., 1971. The bands in the region of 420–500 cm^{-1} are related to internal tetrahedron vibrations of Si–O and Al–O of sodalite (T–O–T) bending modes of the sodalite framework. There is an important assignment in the range of 1003–970 cm^{-1} with the literature for the characteristic bands between 1250 and 950 cm^{-1} asymmetric stretching vibration for all the zeolitic materials (Flaningen et al., 1971). The broad band at about 3450 cm^{-1} and a band at 1650 cm^{-1} are attributed to zeolitic water (Fig. 3). The IR spectral analysis results thus support the XRD inferences. The reference IR wave numbers were given as 1003, 662, 553 and 462 cm^{-1} (Markovic et al., 2003). The original IR spectrum of zeolite A sample (Fluka No. 69836) is shown in Fig. 3i.

The obtained products contain quartz impurities which obscure some of the features of the spectra. The band at about 462 cm^{-1}, which is assigned to tetrahedral T–O (T = Si or Al) bending vibrations, is common to the starting metakaolin (Fig. 3a) and to the different obtained products (Fig. 3b–h). Its intensity does not change substantially in the course of zeolitization. A band at 553 cm^{-1}, assigned to external linkages, is characteristic of zeolite A (Flaningen et al., 1971). Weak bands at about 533 and 1035 cm^{-1} is characteristic of zeolite A, which was obtained at 1.0 M NaOH (Fig. 3b). It appears that in addition to some zeolite A, this product contains greater unchanged metakaolin than the other obtained products (Fig. 3c–h), in agreement with the XRD patterns, in which unchanged metakaolin was detected together with zeolite A. The IR spectra at 1.5 M NaOH (Fig. 3c) were similar to those obtained at 2.0 and 2.5 M NaOH concentrations (Fig. 3d and e). In these products, the absorption at about 1003 cm^{-1} is common to zeolite A and appears as a weak shoulder due to the large amount of quartz present in minor amounts.

The IR spectra at 3.0 and 3.5 M NaOH concentrations correspond to those presented by Flaningen et al. (1971) for zeolite A and the commercial zeolite A (Fig. 3i) except for the contribution of impurities such as quartz (Fig. 3f and g). The IR spectra at 4.0 M NaOH (Fig. 3h) showed that the common shoulder of zeolite A was shifted to 996 cm^{-1} and with differences in 462, 553, 662 cm^{-1} shoulders compared to other obtained zeolite products (Fig. 3). Evidentially the obtained product with 4.0 M NaOH contained a significantly lower portion of zeolite A than any other products obtained by reaction with NaOH concentrations from 1.5 to 3.5 M (Fig. 3) On the other hand, a higher proportion of hydroxysodalite was detected (Table 2), which could account for the decrease in the amount of zeolite A.

3.3. Scanning electron microscopy (SEM) results

SEM micrographs (Fig. 4) show the occurrences of the zeolitic products obtained after hydrothermal treatment of metakaolin in various NaOH concentrations, revealing a marked change in the morphology of the original surface of the starting materials. Kaolinite can be recognized by its platy morphology and

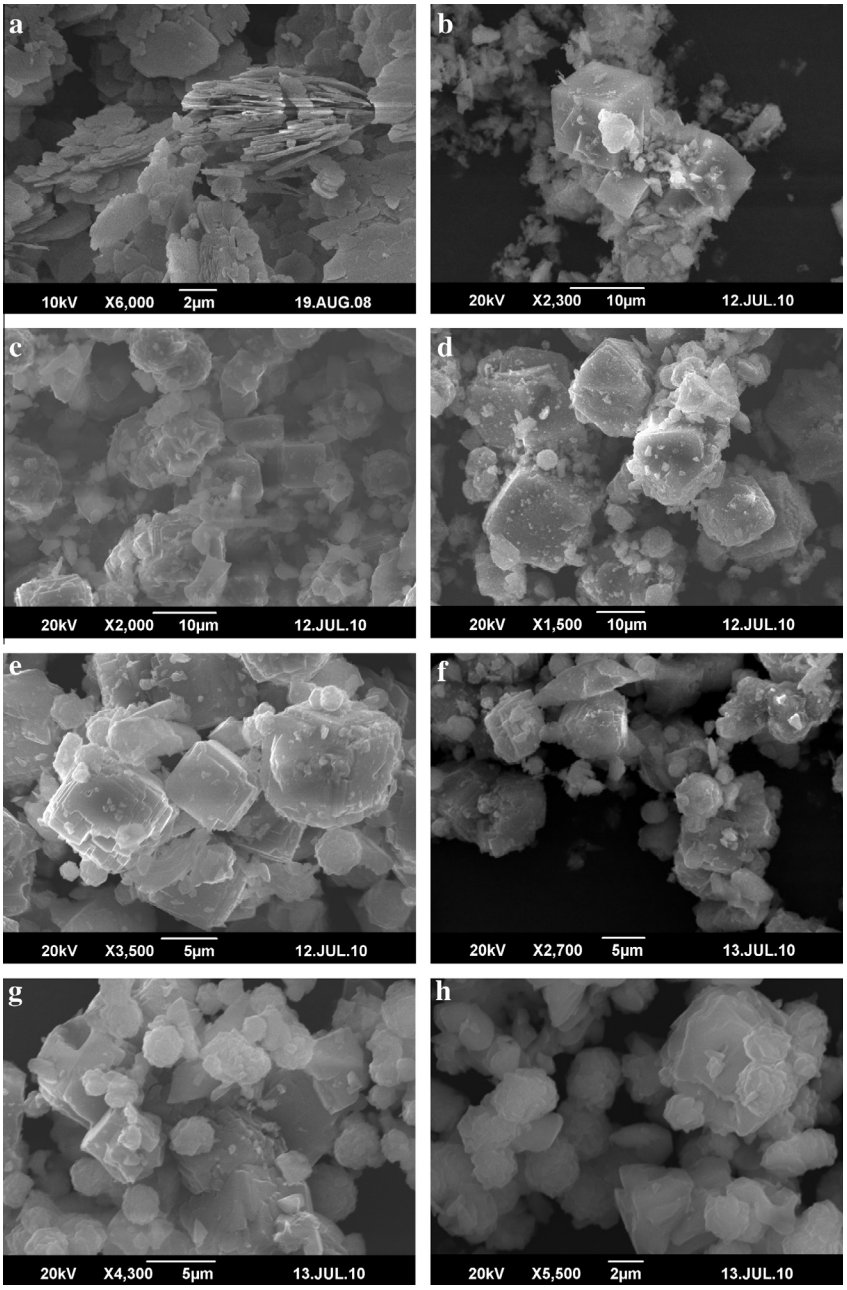

Figure 4 SEM micrographs showing the occurrence of zeolite A and associated phases obtained by hydrothermal synthesis: (a) hexagonal platy crystals of untreated kaolin, (b) very well developed cubes of zeolite A and relicts of metakaolin, (c) zeolite A probably formed before hydroxysodalite (HS), as shown by the occurrence of HS crystals growing at the surface of zeolite A. (d–f) Spheroidal aggregates of HS that grew out onto the surface of cubic crystals of zeolite A, showing penetration twining, and (g–h) lephispheric morphology of HS associated to cubic crystals of zeolite.

hexagonal outlines (Fig. 4a). In accordance with the results of other analytical methods quartz can be detected even by SEM in each sample (see Table 2).

Fig. 4(b–h) represents the effect of different NaOH concentrations (1.0, 1.5, 2.0, 2.5, 3.0, 3.5 and 4.0 M NaOH) on zeolite A formation obtained after activation of metakaolin at 100 °C for 20 h. According to the experimental results of this work, the observed morphologies are similar to those reported in previous studies (Heller-Kallai and Lapides, 2007; Lapides and Heller-kallai, 2007) and the data obtained by SEM correlate and agree with the mineralogical composition of the zeolite products, which was determined through XRD results (Fig. 2 and Table 2).

At 1.0 M NaOH concentration, very well developed cubes of zeolite A as well as a large amount of metakaolin debris were observed in the scanned sample (Fig. 4b). At 1.5 M NaOH solution, zeolite A can be identified by its characteristic cubic morphology (Fig. 4c); it probably formed before hydroxysodalite (HS), as shown by the occurrence of HS crystals growing at the surface of zeolite A.

Lephispheric morphologies corresponding to HS grew out onto the surface of cubic crystals of zeolite A, which sometimes display interpenetrating twining (Fig. 4d–f), which were obtained at 2.0–3.0 M NaOH concentrations. Generally, it is possible to observe the following relationships between these phases: crystal of HS growing at the surface of a cubic crystal of zeolite A, aggregates of spheroidal "cotton-ball" structure of HS along with cubic crystals of zeolite A.

By increasing the NaOH concentrations from 3.5 to 4.0 M, SEM micrographs of treated metakaolin show that a predominantly lephispheric morphology is typically observed in the obtained zeolitic products with spheroidal "cotton-ball" morphologies for HS (Fig. 4g and h).

4. Conclusions

Based on the results of XRD, IR and SEM of zeolite A produced by treating the activated metakaolin from natural Jordanian kaolin with various concentrations of NaOH at 100 °C for 20 h, some observations could be summarized as follows:

- The results indicated that the obtained zeolite products contain zeolite A as the major constituent phase, whereas hydroxysodalite (HS) and quartz were found as minor phases. With one exception untransformed metakaolin occurred only in considerable amounts at 1.0 M NaOH (Table 2). Although the amount of untransformed metakaolin probably decreases with increasing NaOH concentration. On the other hand, amount of HS increases with the increasing NaOH concentration, which could account for the decrease in the amount of zeolite A.
- The synthesized products were found to contain quartz phases as impurities coming from the natural kaolin samples (see XRD pattern in Fig. 1a).
- Zeolite A was hydrothermally synthesized using kaolin as the raw material. The XRD analysis confirmed an excellent relative crystallinity. The surface morphology was proven to be cubic by SEM. Kaolin was suggested to be a feasible and economical raw material for the practical industrial production of zeolite A.
- For a future research we are going to evaluate the efficiency of such zeolite materials in selective cation exchange as ion exchangers, adsorbents and catalysts.

Acknowledgments

The authors are grateful to the Tafila Technical University (TTU) and the German Sciences Foundation "Deutsche Forschungsgemeinschaft" (DFG) for financially supporting this study. Special thanks to Prof. C. Ruscher and Dr. Lars Robben for assistance with the acquisition of FTIR, and SEM data, respectively, as well as three anonymous reviewers for constructive comments on the manuscript.

References

Adamczyk, Z., Bialecka, B., 2005. Hydrothermal synthesis of zeolites from polish coal fly ash. Pol. J. Environ. Stud. 14 (6), 713–719.

Akolekar, D., Chaffee, A., Howe, R., 1997. The Transformations of Kaolin to Low-Silica X Zeolite. Zeolites 19 (5), 359–365.

Alberti, A., Colella, C., Oggiano, G., Pansini, M., Vezzalini, G., 1994. Zeolite production from waste kaolin containing materials. Mater. Eng. (Modena, Italy) 5, 145–158.

Alkan, M., Hopa, C., Yilmaz, Z., Guler, H., 2005. The effect of alkali concentration and solid/liquid ratio on the hydrothermal synthesis of zeolite NaA from natural kaolin. Microporous Mesoporous Mater. 86, 176–184.

Barnes, M.C., Addai-Mensah, J., Gerson, A.R., 1999a. The mechanism of the sodalite-to- cancrinite phase transformation in synthetic spent bayer liquor. Microporous Mesoporous Mater. 31, 287–302.

Barnes, M.C., Addai-Mensah, J., Gerson, A.R., 1999b. A methodology for quantifying sodalite and cancrinite phase mixtures and the kinetics of the sodalite to cancrinite phase transformation. Microporous Mesoporous Mater. 31, 303–319.

Barnes, M.C., Addai-Mensah, J., Gerson, A.R., 1999c. The solubility of sodalite and cancrinite in synthetic spent bayer liquor. Colloids Surf. A Physicochemical and Engineering Aspects 157, 106–116.

Barrer, R.M., 1978. Zeolites and Clay Minerals as Sorbents and Molecular Sieves. Academic Press, London.

Bauer, A., Berger, G., 1998. Kaolin and smectite dissolution rate in high molar KOH solutions at 35° and 80 °C. Appl. Geochem. 13, 905–916.

Bauer, A., Velde, B., Berger, G., 1998. Kaolin transformation in high molar KOH solutions. Appl. Geochem. 13, 619–629.

Bekkum, V.H., Flanigen, E.M., Jacobs, P.A., Jansen, J.C., 1991. Introduction to Zeolite Science and Practice, 2nd revised Ed. Elsevier, Amsterdam.

Breck, D.W., 1974. Zeolite Molecular Sieves: Structure, Chemistry and Uses. John Wiley, New York.

Buhl, J.C., 1991. Synthesis and characterization of the basic and non-basic members of the cancrinite-natrodavyne family. Thermochim. Acta 178, 19–31.

Buhl, J.C., Loens, J., 1996. Synthesis and crystal structure of nitrate enclathrated sodalite $Na_8[AlSiO_4]_6(NO_3)_2$. J. Alloys Compd. 235, 41–47.

Buhl, J.C., Stief, F., Fechtelkord, M., Gesing, T.M., Taphorn, U., Taake, C., 2000a. Synthesis, X-ray diffraction and MAS NMR characteristics of nitrate cancrinite $Na_{7.6}$ $[AlSiO_4]6(NO_3)$ $1.6(H_2O)_2$. J. Alloys Compd. 305, 93–102.

Buhl, J.C., Hoffmann, W., Buckermann, W.A., Muller-Warmuth, W., 2000b. The crystallization kinetics of sodalites grown by the hydrothermal transformation of kaolin studied by 29Si MAS NMR. Solid State Nucl. Magn. Reson. 9, 121–128.

Covarrubias, J.C., Garcia, R., Arriagada, R., Yanez, J., Garland, T., 2006. Cr(III) Exchange on Zeolites Obtained from Kaolin and Natural Mordenite. Microporous Mesoporous Mater. 88, 220–231.

Dudzik, Z., Kowalak, S., 1974. Preparation of zeolites of faujasite type from kaolin. Przemys'I Chemiczny 53, 616–618.

Earl, D.J., Deem, M.W., 2006. Toward a database of hypothetical zeolite structures. Ind. Engendering Chem. Res. 45, 5449–5454.

Engelhardt, G., Michel, D., 1987. High-Resolution Solid-State NMR of Silicates and Zeolites. Wiley, New York.

Fialips, G.C., 1999. Etude expeérimentale de la cristallinité et des conditions deformation de la kaolin. These Doct univ Poitiers France.

Flaningen, E.M., Khatami, H.A., Szymanski, H.A., 1971. Mol. Sieve Zeolites 16, 201.

Gougazeh, M., Buhl, J.-C.h., 2010. Geochemical and Mineralogical Characterization of the Jabal Al-Harad Kaolin Deposit, Southern Jordan for its Possible Utilization. Clay Miner. Mineral. Soc. Great Britain Ireland 45 (4), 281–294.

Gualtieri, A., Norby, P., Artioli, G., Hanson, J., 1997. Kinetic study of hydroxysodalite formation from natural kaolins by time-resolved synchrotron powder diffraction. Microporous Mater. 9, 189–201.

Heller-Kallai, L., Lapides, I., 2007. Reactions of kaolin and metakaolins with NaOH – comparison of different samples (Part 1). Appl. Clay Sci. 35, 99–107.

Lapides, I., Heller-Kallai, L., 2007. Reactions of metakaolin with NaOH and colloidal silica – comparison of different samples (Part 2). Appl. Clay Sci. 35, 94–98.

Loewenstein, W., 1954. Am. Miner. 39, 92.

Lin, D.C., Xu, X.W., Zuo, F., Long, Y.C., 2004. Crystallization of JBW, CAN, SOD and ABW type zeolite from transformation of metakaolin. Microporous Mesoporous Mater. 70, 63–70.

Lin, C., His, H., 1995. Environ. Sci. Technol. 29, 1748–1753.

Loiola, A.R., Andrade, J.C.R.A., Sasaki, J.M., da Silva, L.R.D., 2012. Structural analysis of zeolite NaA synthesized by a cost-effective hydrothermal method using kaolin and its use as water softener. J. Colloid Interface Sci. 367, 34–39.

Marcelo, L.M., Diego, I.P., Nadia, R.C., Fernandes.Machado, Sibele, B.C., Pergher,, 2007. Synthesis of mordenite using kaolin as Si and Al source. Appl. Clay Sci. 41, 99–104.

Markovic, S., Dondur, V., Dimitrijevic, R., 2003. J. Mol. Struct. 654, 223–234.

McCusker, L.B., Baerlocher, C., 2001. Zeolite structures. In: Van Bekkum, H., Flanigen, E.M., Jacobs, P.A., Jansen, J.C. (Eds.), Introduction to zeolite science and practice Studies in Surface Science and Catalysis, vol. 137. Elsevier, Amsterdam, pp. 37–65.

Mon, J., Deng, Y., Flury, M., Harsh, J., 2005. Cesium incorporation and diffusion in cancrinite, sodalite, Zeolite, and allophone. Microporous Mesoporous Mater. 86, 277–286.

Murray, H.H., 1991. Overview: Clay Mineral Application. Appl. Clay Sci. 5, 379–395.

Nesse, W.D., 2000. Introduction of mineralogy. Oxford University Press.

Querol, X., Plana, F., Alastuey, A., Lopez-Soler, A., 1997. Synthesis of Na-zeolites from fly ash. Fuel 76, 793–799.

Rees, L., Chandrasekhar, S., 1993. Hydrothermal reaction of kaolin in presence of fluoride ions at pH less than 10. Zeolites 13, 534–541.

Rios, C.A., Williams, C.D., Maple, M.J., 2007. Synthesis of zeolites and zeotypes by hydrothermal transportation of kaolinite and metakaolinite. BISTUA 5 (1), 15–26.

Saija, L.M., Ottana, R., Zipelli, C., 1983. Zeolitization of pumice in ash-sodium salt solutions. Mater. Chem. Phys. 8, 207–216.

Sandoval, M.V., Henao, J.A., Rios, C.A., Williams, C.D., Apperley, D.C., 2009. Synthesis and characterization of zeotype ANA framework by hydrothermal reaction of natural clinker. Fuel 88, 272–281.

Sanhueza, V., Kelm, U., Cid, R., 1999. Synthesis of molecular sieves from Chilean kaolins: 1. Synthesis of NaA type zeolite. J. Chem. Technol. Biotechnol. 74, 358–363.

Singer, A., Berkgaut, V., 1995. Environ. Sci. Technol. 29, 1748–1753.

Smykatz-Kloss, W., 1975. Differential Thermal Analysis, Application and Results in Mineralogy. Springer, New York.

Szoztak, R., 1998. Molecular Sieves: Principles of Synthesis and Identification, 2nd ed. Blackie Academic and Professional, London, 359 pp.

Takaishi, T., Kato, M., Itabashi, K., 1995. Determination of the ordered distribution of aluminum atoms in a zeolitic framework. Part II. Zeolites 15, 21–32.

Tanaka, H., Miyagawa, A., Eguchi, H., Hino, R., 2004. Synthesis of a pure-form Zeolite A from coal fly ash by dialysis. Ind. Eng. Chem. Res. 43, 6090–6094.

Treacy, M.J., Higgins, J.B., 2001. Collections of Simulated XRD Powder Patterns for Zeolites, 4th ed. Elsevier, Amsterdam, The Netherlands, 379 p.

Walek, T.T., Saito, F., Zhang, Q., 2008. The effect of low solid/liquid ratio on hydrothermal synthesis of zeolites from fly ash. Fuel 87, 3194–3199.

Vilma, S., Ursula, K., Ruby, C., 1999. Synthesis of molecular sieves from Chilean kaolins: 1. synthesis of NaA type zeolites. J. Chem. Technol. Biotechnol. 74, 358–363.

Wang, C.F., Li, J.S., Wang, L.J., Sun, X.Y., 2008. Influence of NaOH concentrations on synthesis of pure-form zeolite A from fly ash using two-stage method. J. Hazard. Mater. 155, 58–64.

Zhao, H., Deng, Y., Harsh, J., Flury, M., Boyle, J., 2004. Alteration of Kaolinite to Canrinite and Sodalite by Simulated Hanford Waste and its Impact on Cesium Retention. Calys Clay Miner. 52 (1), 1–13.